Hybrid Quantum-Classical Approach to Quantum Optimal Control

Jun Li,[1,*] Xiaodong Yang,[2] Xinhua Peng,[2,3,†] and Chang-Pu Sun[1]
[1]*Beijing Computational Science Research Center, Beijing 100193, China*
[2]*Hefei National Laboratory for Physical Sciences at Microscale and Department of Modern Physics, University of Science and Technology of China, Hefei, Anhui 230026, China*
[3]*Synergetic Innovation Centre of Quantum Information & Quantum Physics, University of Science and Technology of China, Hefei, Anhui 230026, China*
(Received 10 August 2016; revised manuscript received 19 January 2017; published 11 April 2017)

A central challenge in quantum computing is to identify more computational problems for which utilization of quantum resources can offer significant speedup. Here, we propose a hybrid quantum-classical scheme to tackle the quantum optimal control problem. We show that the most computationally demanding part of gradient-based algorithms, namely, computing the fitness function and its gradient for a control input, can be accomplished by the process of evolution and measurement on a quantum simulator. By posing queries to and receiving answers from the quantum simulator, classical computing devices update the control parameters until an optimal control solution is found. To demonstrate the quantum-classical scheme in experiment, we use a seven-qubit nuclear magnetic resonance system, on which we have succeeded in optimizing state preparation without involving classical computation of the large Hilbert space evolution.

DOI: 10.1103/PhysRevLett.118.150503

Quantum computing promises to deliver a new level of computation power [1]. Enormous efforts have been made in exploring the possible ways of using quantum resources to speed up computation. While the fabrication of a full-scale universal quantum computer remains a huge technical challenge [2], special-purpose quantum simulation can be an alternative [3–5]. Quantum simulators are designed to imitate specific quantum systems of interest, and are expected to provide significant speed-up over their classical counterparts [6]. In recent years, quantum simulation has found important applications for a great variety of computational tasks, such as solving linear equations [7,8], simulating condensed-matter systems [9], calculating molecular properties [10,11], and certificating untrusted quantum devices [12]. However, in view of experimental implementation, most of the proposed algorithms have hardware requirements still far beyond the capability of near-term quantum devices.

Recent advances towards building a modest-sized quantum computer have led to emerging interest in a quantum-classical hybrid approach [13–15]. The underlying idea is that by letting a quantum simulator work in conjunction with a classical computer, even minimal quantum resources could be made useful. In hybrid quantum-classical computation, the computationally inexpensive calculations, which yet might consume many qubits, are performed on a classical computer, whereas the difficult part of the computation is accomplished on a quantum simulator. The major benefit of this hybrid strategy is that it gives rise to a setup that can have much less stringent hardware requirements.

In this Letter, we propose a hybrid quantum-classical method for solving the quantum optimal control problem. Normally, the problem is formulated as follows: given a quantum control system and a fitness function that measures the quality of control, the goal is to find a control that can achieve optimal performance. The importance of the problem lies in its extraordinarily wide range of applications in physics and chemistry [16]. However, current numerical approaches suffer from the scalability issue as they involve computation of the many time propagations of the state of the controlled system, which can be infeasible on classical computers for systems of large dimensions [17]. To address this computational challenge, we develop hybrid quantum-classical versions of gradient-based optimal control algorithms [18]. We show that, given a reliable quantum simulator that efficiently simulates the controlled quantum evolution, then under certain reasonable conditions this simulator can be used to efficiently estimate both the fitness function and its gradient. Additionally, a classical computer is employed to store the control parameters as well as to determine the search direction in each iteration according to the gradient information that it receives from the simulator. Working in such a quantum-classical manner, there can be expected a significant saving of memory cost and time cost and hence an enhancement of the ability of solving the quantum optimal control problem for large-sized quantum systems.

The proposed hybrid scheme is amenable to experimental implementation with current state-of-the-art quantum technology. Here, we also report a first experimental realization of the scheme on a nuclear magnetic resonance (NMR) system. The experimental results show excellent performance of our method in obtaining high-quality optimal control solutions.

Theory.—To start, we briefly describe the quantum state engineering problem. Consider an n-spin-1/2 quantum spin system, which evolves under a local Hamiltonian $H_S = \sum_l^L H_l$. Here, each of the L terms H_l acts on a subsystem containing at most a constant number of spins. Such a form of Hamiltonian can be efficiently simulated [19] and can describe a variety of quantum systems, e.g., the quantum Ising model and the Heisenberg model. Suppose the system is manipulated with a transverse time-varying magnetic control field $u(t) = (u_x(t), u_y(t)) : t \in [0, T]$. Let σ_x, σ_y, and σ_z denote the Pauli operators, then the control Hamiltonian reads $H_C(t) = \sum_{k=1}^n (u_x(t)\sigma_x^k + u_y(t)\sigma_y^k)$, in which $\hbar$ is set as 1 and the gyromagnetic ratios are not written explicitly. The control task is to steer the system between states of interest in the Liouvillian space. Normally, we need a fitness function to give a performance metric of the control. To this end, a set of operators $\mathcal{P}_n = \{P_k\}_{k=0}^{4^n-1} = \{I, \sigma_x, \sigma_y, \sigma_z\}^{\otimes n}$, with I being the 2×2 identity, is introduced. It constitutes an orthonormal basis of the state space: $\mathrm{Tr}(P_k P_j)/2^n = \delta_{kj}$ for $k, j = 0, \ldots, 4^n - 1$. Thus, any state can be represented as a vector with respect to $\mathcal{P}_n$. Let the system's starting point be ρ_i and the target be $\bar{\rho} = \sum_{s \in S} x_s P_s$, where S is the index set for s. As we are considering closed system engineering, ρ_i should be unitarily convertible to $\bar{\rho}$. Now the state-to-state transfer task is formulated as the quantum optimal control problem [18],

$$\begin{aligned} \max \quad & f[U(T)\rho_i U(T)^\dagger, \bar{\rho}] = \mathrm{Tr}[U(T)\rho_i U(T)^\dagger \cdot \bar{\rho}]/2^n, \\ \text{s.t.} \quad & \dot{U}(t) = -i\left(H_S + \sum_{k=1}^n (u_x(t)\sigma_x^k + u_y(t)\sigma_y^k)\right) U(t), \end{aligned}$$

where $U(0) = I^{\otimes n}$ and f, the fitness function, is expressed as a functional of the input control $u(t)$ and may possess many local extrema. Except for relatively small systems with two or three qubits [20,21], analytically solving the problem for generic H_S is difficult.

Generally, one must resort to numerical investigations, and the most favored approach is to employ gradient-based optimization methods. A gradient-based algorithm generates a sequence of iterates $u^{(0)}, u^{(1)}, \ldots$, which starts from a designed trial input or even simply a random guess, and stops when a certain termination condition is fulfilled [22]. The move from one iterate $u^{(q)}$ $(q \geq 0)$ to the next follows the line search strategy

$$u^{(q+1)} = u^{(q)} + \alpha^{(q)} p^{(q)}, \tag{1}$$

that is, it first fixes a search direction $p^{(q)}$ and then identifies a move distance $\alpha^{(q)}$ along that direction. The computation of $p^{(q)}$ makes use of information about f and the gradient ∇f at current iterate $u^{(q)}$, and possibly also information from earlier iterates. The step size $\alpha^{(q)}$ is chosen such that a sufficient increase in f can be acquired. The algorithm succeeds if the sequence $f(u^{(0)}), f(u^{(1)}), \ldots$ converges to a desired local extremum. There exist various types of gradient-based algorithms, which are classified based on the method used for determining the search direction. For example, the known gradient ascent pulse engineering (GRAPE) [18] algorithm finds local extrema by taking steps proportional to the gradient, while conjugated gradient [23] and quasi-Newton methods [24] would search along other gradient-related directions that allow for faster convergence speed.

Here we develop a hybrid quantum-classical framework for gradient-based optimal control. It would be convenient to cast the ideas in terms of the standard oracle-based optimization model [25,26]. Consider an oracle function $\mathcal{O} : u \to \{f(u), \nabla f(u)\}$ which, when queried at any point u, gives the corresponding value of f and ∇f. Obviously, constructing such an oracle $\mathcal{O}$ represents the most computationally resource-consuming part of the optimization procedure, and we propose to realize it with using a reliable quantum simulator. The simulator does not necessarily have to be universal. For instance, it can just be provided by the controlled system itself [27–29]. The simulator works with a classical computer that stores the control variables and records all iterative information if necessary. Our hybrid scheme consists of successive rounds of control updates; see Fig. 1. For each round the classical computer first sends the current point u to the oracle $\mathcal{O}$ as input, meaning that it is posing a query, and then, according to the answer of $\mathcal{O}$, it executes a line search subroutine so as to decide at which point the next query should be made. Here, the query is encoded in control pulses and the answer is extracted through quantum measurements on the final state of the simulator.

So far we have not mentioned the convergence properties of the optimization. Gradient-based algorithms may get trapped at suboptimal points. Yet research shows that, under certain conditions, most of the control landscapes are trap free and convergence to an optimal solution is usually fast [30]. In our hybrid quantum-classical scheme, the only change is that we use quantum resources to implement the oracle function $\mathcal{O}$. Therefore, the convergence properties will remain unchanged as long as our quantum simulator is sufficiently trustable.

Now we explain how the oracle $\mathcal{O}$ is quantumly constructed. We use the number of experiments needed to compute $\mathcal{O}$ as a complexity measure of the method. Running the numerical optimization requires that the control field be discretized. Let the pulse $u(t)$ be divided into M slices with each time slice being of constant magnitude and fixed length $\tau = T/M$. In consideration of memory cost, M should be polynomially scaled. The mth slice control $u[m]$ generates the propagator

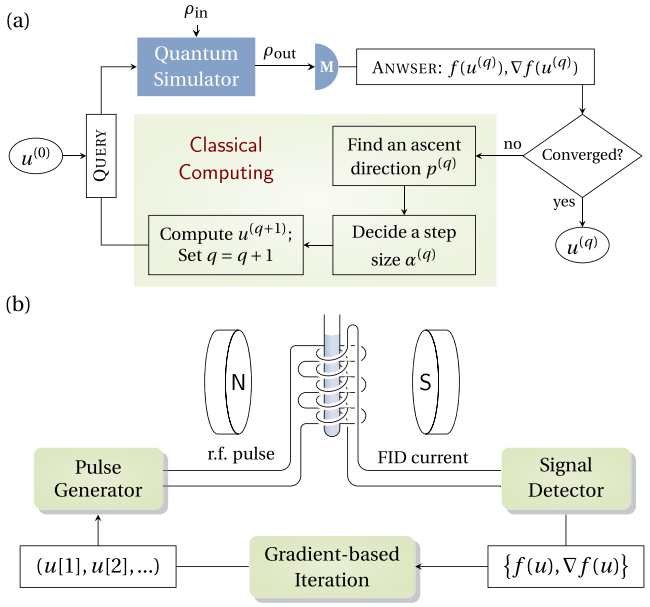

FIG. 1. (a) Hybrid quantum-classical approach to gradient-based optimal control iterative algorithms, wherein the quantum simulator is combined with classical computing devices to jointly implement the procedure of optimal control searching. Here, ρ_{in} is the input state, ρ_{out} is the output state, double-lined arrows signify quantum information, and **M** represents quantum measurement. (b) Schematic diagram of an NMR based implementation of the quantum-classical hybrid optimal control searching. The sample consists of an ensemble of spins and serves as a quantum processor. Query is encoded in input radio-frequency (rf) control pulse and the answer that the sample generates is extracted from observing the free induction decay (FID).

$$U_m = \exp\left\{-i\left[H_S + \sum_{k=1}^{n}(u_x[m]\sigma_x^k + u_y[m]\sigma_y^k)\right]\tau\right\}.$$

For notational brevity let $U_{m_1}^{m_2}$ denote $U_{m_2}\cdots U_{m_1+1}U_{m_1}$, where $m_2 \geq m_1$. So the final state is $\rho_f = U_1^M \rho_i U_1^{M\dagger}$. We, hence, have the following expression for f:

$$f = \mathrm{Tr}(\rho_f\bar{\rho})/2^n = \sum_{s\in S} x_s \mathrm{Tr}(\rho_f P_s)/2^n. \quad (2)$$

It can be readily seen from the equation that, rather than full tomography of final state, f can be directly measured with $|S|$ experiments. That is, for the sth experiment we first initialize our simulator at ρ_i, then simulate the system evolution under control u and then measure the final state with basis operator P_s. After this, we sum up all the measurement results according to Eq. (2) and hence obtain an estimation of f.

Next, let us see how to compute the $2M$-dimensional gradient vector $g = \nabla f = (g_x[m], g_y[m])$, where $g_\alpha[m] = \partial f/\partial u_\alpha[m]$ ($\alpha = x$ or y). To first order approximation, it is evaluated as [18]

$$g_\alpha[m] = \sum_{k=1}^{n} \mathrm{Tr}(-i\tau U_{m+1}^M[\sigma_\alpha^k, U_1^m \rho_i U_1^{m\dagger}]U_{m+1}^{M\dagger}\bar{\rho})/2^n. \quad (3)$$

The approximation is good if τ is sufficiently small. Note that for any operator ρ, there is

$$[\sigma_\alpha^k, \rho] = i\left[R_\alpha^k\left(\frac{\pi}{2}\right)\rho R_\alpha^k\left(\frac{\pi}{2}\right)^\dagger - R_\alpha^k\left(-\frac{\pi}{2}\right)\rho R_\alpha^k\left(-\frac{\pi}{2}\right)^\dagger\right], \quad (4)$$

in which $R_\alpha^k(\pm\pi/2)$ is the $\pm\pi/2$ rotation about the α axis on the kth qubit. The essential point is that we can compute the commutator by means of local qubit rotations. Substituting Eq. (4) into Eq. (3), one gets that

$$g_\alpha[m] = \tau\sum_{k=1}^{n}[\mathrm{Tr}(\rho_{\alpha_+}^{km}\bar{\rho}) - \mathrm{Tr}(\rho_{\alpha_-}^{km}\bar{\rho})]/2^n, \quad (5)$$

where $\rho_{\alpha_\pm}^{km} = U_{m+1}^M R_\alpha^k(\pm\pi/2)U_1^m\rho_i(U_{m+1}^M R_\alpha^k(\pm\pi/2)U_1^m)^\dagger$. Therefore, to obtain the mth component of g_α, we perform $2n$ experiments: we (i) sequentially take out an element from the operation set $\{R_\alpha^k(\pm\pi/2)\}_{k=1,\ldots,n}$, and insert it after the mth slice evolution; (ii) measure the distances of the final states with respect to $\bar{\rho}$, and (iii) combine all the measurement results according to Eq. (5). A quick calculation shows that in each round of iteration in total $4nM|S|$ experiments are needed to perform gradient estimation.

Summarizing the above derivations, we conclude that in total we need to perform $(4nM+1)|S|$ experiments on the quantum simulator to estimate f and g. It is interesting to seek instances for which our scheme can be qualitatively advantageous over conventional approaches. Obviously, that target states possessing exponential number of nonzero components require also that many measurements to take. This implies that, to ensure the whole process be feasible, we have to restrict consideration to a specific kind of target states. An important fact in quantum computing says that, to build up quantum operations out of a small set of elementary gates is generically inefficient [1]. In other words, there are overwhelmingly many states that are complex in the sense that they take the exponential size of a quantum circuit to approximate. Therefore, it makes sense if we restrict ourselves to relatively less complicated states, for example, those which admit sparse representation with respect to some basis, where the basis fulfils the condition that measurement of any of its elements consumes only polynomial resources. In the present setting, we will be interested in $|S|$-sparse states under basis $\mathcal{P}_n$ with $|S| \ll |\mathcal{P}_n|$. Despite the problem simplification, from the practical side they are undoubtedly still difficult tasks at the current level of large-system control technology. The sparsity assumption drastically reduces the time cost for physically implementing $\mathcal{O}$ and, consequentially, the great chance of our hybrid quantum-classical approach to provide significant speedup.

Experiment.—We choose the fully ^{13}C-labeled crotonic acid as our test system, on which we demonstrate the idea of using the sample to compute its own optimal control pulse. The sample consists of four carbon nuclei and five proton nuclei, in which the methyl protons H_3, H_4, and H_5 are chemically and magnetically equivalent and hence are indistinguishable; see Fig. 2(a). Therefore, the nine physical spins map onto seven addressable qubits, where one of these qubits is obtained from the subsystem of methyl spins. Experiment is carried on a Bruker Avance III 400 MHz spectrometer at room temperature. The system Hamiltonian takes the form $H_S = \sum_{k=1}^{n} \Omega_k \sigma_z^k/2 + \pi \sum_{k<j}^{n} J_{kj} \sigma_z^k \sigma_z^j/2$, where Ω_k is the precession frequency of the kth spin, and J_{kj} is the coupling between the kth and jth spin; see Supplemental Material [31] for their values. To describe states of the nuclei, we use deviation density matrices, that is, the traceless part of the density matrices up to an overall scale [32]. Our goal is to create state $\bar{\rho} = \sigma_z^1 \sigma_z^2 \sigma_z^3 \sigma_z^5 \sigma_z^7 \sigma_z^8 \sigma_z^9$, which is the largest multiple-spin correlated operator that can be directly observed from the spectrum. Observation is made on C_2 because all the couplings are adequately resolved. Our experiment is divided into two parts: reset and preparation.

In the reset part we return the system to a fixed initial state ρ_i, which has to be unitarily equivalent to $\bar{\rho}$. So the system's equilibrium state is not considered because it has different spectra with that of $\bar{\rho}$. Although there are many candidates, we choose $\rho_i \propto \sigma_z^2$ for convenience of observation. Figure 2(b) shows our initialization sequence design. First, we apply a continuous wave (cw) on the proton channel. Because of the steady state heteronuclear Overhauser effect (NOE) [33], provided that the cw irradiation is sufficiently long and strong, the system will be driven asymptotically into a steady state ρ_{ss} of the form $\rho_{ss} = \sum_{k=1}^{4} \epsilon_{ss}^k \sigma_z^k$, that is, the protons are saturated. In experiment, the irradiation is set to be 10 s duration and 2500 Hz magnitude. As expected, we see the establishment of the steady state, in which only the carbons' polarizations are left, but with enhanced bias compared to the equilibrium state. For example, the NOE enhancement factor of C_2 is about 1.8. Next, we retain just the signal of C_2 by first rotating the polarizations of other carbons to the transverse plane and then destroying them with z-axis gradient field. This gives the desired initial state ρ_i.

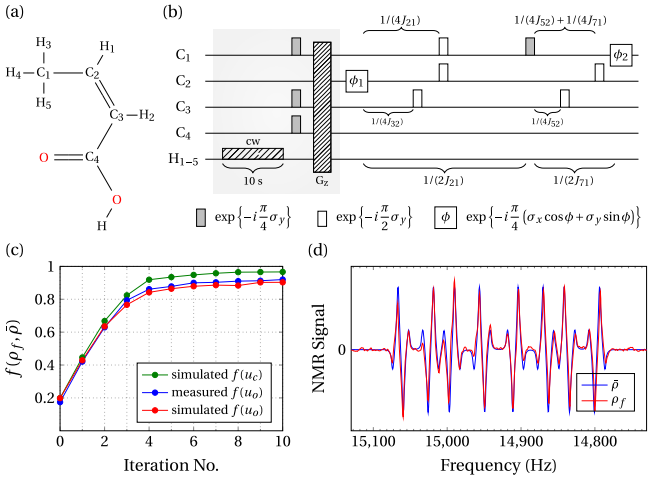

FIG. 2. (a) Molecular structure of crotonic acid. (b) Pulse sequence scheme for our multiple-quantum coherence generation experiment. The gray part is designed to reset the system back into ρ_i, and the preparation part is an approximate circuit (in which cw: continuous wave; G_z: gradient pulse along z axis; $\phi_1 = -18°$ and $\phi_2 = 82°$) aimed for making the transform $\rho_i \to \bar{\rho}$. (c) Iterative results for our system. Here u_c and u_o denote the controls obtained by searching on a classical computer and on the sample, respectively. (d) NMR spectrum of ρ_f after 10 times of iteration under the observation of C_2. It is placed with the simulated ideal spectrum of target state $\bar{\rho}$ together for comparison.

The preparation part aims to steer ρ_i towards $\bar{\rho}$. To give a good initial control guess to accelerate convergence, we designed an approximate preparation circuit. The approximate circuit is constructed based on a simplified system Hamiltonian which ignores the small couplings and the small differences between large couplings of the original Hamiltonian. Such simplification manifests which couplings are allowed to evolve for preparing $\bar{\rho}$, and thus enables direct circuit construction; see Fig. 2(b). The circuit thus constructed, if we turn back to the real Hamiltonian, generates a final state that deviates $\bar{\rho}$ only slightly: $f \approx 0.9824$. Moreover, the circuit length is 16.36 ms, much shorter than the system's relaxation time, so the preparation stage can be taken as unitary. In order that the number of control parameters after pulse discretization be as few as possible, we adopt a relatively large time step length $\tau = 20\ \mu$s. We use Gaussian shaped selective pulses to implement the rotational gates. Each selective pulse has its pulse width determined according to which qubit it is acting on. Excluding the free J evolutions, we have in total 2×108 nonzero pulse parameters to be optimized. We have employed a compilation procedure [34,35] to systematically reduce the errors that come in when the ideal rotational operations are implemented through soft selective pulses, yet f still drops severely. Therefore, some extent of pulse optimization is necessary.

We add a small amount of random disturbances to the above constructed selective pulse network. The purpose of doing so is to start the oracle iteration from a relatively low-quality control and hence to witness a more notable rising of f. According to our previous analysis, we roughly figure out the experiment time cost for each round of iteration to be about 5 h. We have demonstrated the query action on the sample for 10 times. Figures 2(c)–2(d) show the experimental results, from which we see clearly that the successively updated pulse is indeed approaching a solution of the optimal control problem. Because measurement inaccuracies induce errors in gradient estimation, it

is expected that some degree of deviation of the experimental growth of f from that performed on a classical computer appears. Therefore, the important challenge left open is to understand quantitatively how measurement inaccuracies affect the convergence efficiency.

Discussion.—From the control theory perspective, the apparatus in our experiment, including a control input generator, a sample of molecules, and a measurement device, interact as a closed learning loop. In each cycle of the loop, the fitness information learned from the sample directs the optimization to achieve a given control objective. Such strategy has the advantage of reliability and robustness. The learning algorithm is the crucial ingredient, and previous studies have been mainly focused on using stochastic searching strategies such as evolutionary algorithms [36,37]. We here have shown that a large class of gradient-based methods can also be incorporated into the closed loop learning control model. This will be important for realizing high-fidelity quantum control experiments, such as is needed in the fields of quantum information processing and spectroscopy.

Future work will seek to gain a better understanding of the feasibility of the hybrid quantum-classical approach to quantum optimal control. NMR is an excellent platform on which to test various quantum control methods, but for our scheme its drawback is the relatively long reset (relaxation) time. It can be envisioned that on other quantum information processing candidate systems that have much shorter operation time and relaxation time [2], the search process may get several orders of magnitude faster. We expect the methodology developed in this work can promote studies of scalable quantum controls on larger quantum systems.

This work is supported by the National Basic Research Program of China (Grants No. 2014CB921403, No. 2016YFA0301201, No. 2014CB848700 and No. 2013CB921800), National Natural Science Foundation of China (Grants No. 11421063, No. 11534002, No. 11375167 and No. 11605005), the National Science Fund for Distinguished Young Scholars (Grant No. 11425523), and NSAF (Grant No. U1530401).

*lijunwu@mail.ustc.edu.cn
†xhpeng@ustc.edu.cn

[1] M. A. Nielsen and I. L. Chuang, *Quantum Computation and Quantum Information* (Cambridge University Press, Cambridge, England, 2000).
[2] T. D. Ladd, F. Jelezko, R. Laflamme, Y. Nakamura, C. Monroe, and J. L. OBrien, Nature (London) **464**, 45 (2010).
[3] A. M. Childs and W. van Dam, Rev. Mod. Phys. **82**, 1 (2010).
[4] J. I. Cirac and P. Zoller, Nat. Phys. **8**, 264 (2012).
[5] P. Hauke, F. M. Cucchietti, L. Tagliacozzo, I. Deutsch, and M. Lewenstein, Rep. Prog. Phys. **75**, 082401 (2012).
[6] R. P. Feynman, Int. J. Theor. Phys. **21**, 467 (1982).
[7] A. W. Harrow, A. Hassidim, and S. Lloyd, Phys. Rev. Lett. **103**, 150502 (2009).
[8] A. M. Childs, Nat. Phys. **5**, 861 (2009).
[9] G. A. Álvarez, D. Suter, and R. Kaiser, Science **349**, 846 (2015).
[10] B. P. Lanyon *et al.*, Nat. Chem. **2**, 106 (2010).
[11] P. J. J. O'Malley *et al.*, Phys. Rev. X **6**, 031007 (2016).
[12] N. Wiebe, C. Granade, C. Ferrie, and D. G. Cory, Phys. Rev. Lett. **112**, 190501 (2014).
[13] J. R. McClean, J. Romero, R. Babbush, and A. Aspuru-Guzik, New J. Phys. **18**, 023023 (2016).
[14] B. Bauer, D. Wecker, A. J. Millis, M. B. Hastings, and M. Troyer, Phys. Rev. X **6**, 031045 (2016).
[15] S. Bravyi, G. Smith, and J. A. Smolin, Phys. Rev. X **6**, 021043 (2016).
[16] C. Brif, R. Chakrabarti, and H. Rabitz, New J. Phys. **12**, 075008 (2010).
[17] H. J. Hogben, M. Krzystyniak, G. T. P. Charnock, P. J. Hore, and I. Kuprov, J. Magn. Reson. **208**, 179 (2011).
[18] N. Khaneja, T. Reiss, C. Kehlet, T. Schulte-Herbrüggen, and S. J. Glaser, J. Magn. Reson. **172**, 296 (2005).
[19] S. Lloyd, Science **273**, 1073 (1996).
[20] N. Khaneja, R. Brockett, and S. J. Glaser, Phys. Rev. A **63**, 032308 (2001).
[21] A. Carlini, A. Hosoya, T. Koike, and Y. Okudaira, Phys. Rev. A **75**, 042308 (2007).
[22] J. Nocedal and S. J. Wright, *Numerical Optimization* (Springer, New York, 2006).
[23] A. Borzì, J. Salomon, and S. Volkwein, J. Comput. Appl. Math. **216**, 170 (2008).
[24] P. de Fouquieres, S. G. Schirmer, S. J. Glaser, and I. Kuprov, J. Magn. Reson. **212**, 412 (2011).
[25] A. S. Nemirovski and D. B. Yudin, *Problem Complexity and Method Efficiency in Optimization* (Wiley, New York, 1983).
[26] Y. Nesterov, *Introductory Lectures on Convex Optimization: Basic Course* (Springer-Verlag, New York, 2004).
[27] J. Roslund and H. Rabitz, Phys. Rev. A **79**, 053417 (2009).
[28] Q. Sun, I. Pelczer, G. Riviello, R. Wu, and H. Rabitz, Phys. Rev. A **89**, 033413 (2014).
[29] C. Ferrie and O. Moussa, Phys. Rev. A **91**, 052306 (2015).
[30] A. N. Pechen and D. J. Tannor, Phys. Rev. Lett. **106**, 120402 (2011).
[31] See Supplemental Material at http://link.aps.org/supplemental/10.1103/PhysRevLett.118.150503 for more details.
[32] O. W. Sørensen, G. W. Eich, M. H. Levitt, G. Bodenhausen, and R. R. Ernst, Prog. Nucl. Magn. Reson. Spectrosc. **16**, 163 (1984).
[33] M. H. Levitt, *Spin Dynamics: Basics of Nuclear Magnetic Resonance* (John Wiley & Sons Ltd., London, 2008).
[34] C. A. Ryan, C. Negrevergne, M. Laforest, E. Knill, and R. Laflamme, Phys. Rev. A **78**, 012328 (2008).
[35] J. Li, J. Cui, R. Laflamme, and X. Peng, Phys. Rev. A **94**, 032316 (2016).
[36] H. Rabitz, R. de Vivie-Riedle, M. Motzkus, and K. Kompa, Science **288**, 824 (2000).
[37] R. S. Judson and H. Rabitz, Phys. Rev. Lett. **68**, 1500 (1992).